Photodegradation of Polyurethane Foam Obtained from Renewable Resource–Pulp Production Byproducts

A. Paberza[*], L. Stiebra and U. Cabulis

Latvian State Institute of Wood Chemistry, Dzerbenes 27, LV-1006, Riga, Latvia

ABSTRACT: Rigid polyurethane foams were obtained from pulp production byproducts. Three different polyols were used—tall oil polyol, lignopolyol and commercially available polyol for comparison. The obtained rigid polyurethane foams underwent photodegradation at 60°C temperature and at 0.89 W/m^2 intensity of UV light radiation up to 1000 h. Changes in chemical structure were observed by Fourier Transform Infrared Spectroscopy and Scanning Electron Microscopy was used to study changes in cell morphology. Spectrophotometery was used to determine yellowing of the foams. Results showed that the thickness of degraded layer for rigid polyurethane foams obtained from pulp production byproducts was ~25% less than for foams from commercially available polyol. Overall results suggest that rigid polyurethane foams from lignopolyol show better performance against photodegradation.

KEYWORDS: Rigid polyurethane foams, lignopolyol, tall oil polyol, degradation, photodegradation

1 INTRODUCTION

Rigid polyurethane (PUR) foams are a group of polymers with excellent thermal insulation, chemical resistance and toughness combined with good flexibility at low temperatures. Rigid PUR foams are extensively used as insulators in the construction industry, in domestic appliances and refrigerators [1], as well as for transportation of liquefied natural gas and for insulation of cryogenic space launchers [2]. Also, rigid PUR foams have excellent properties such as closed-cell structure, low thermal conductivity, low water adsorption and moisture permeability and relatively high compressive strength. Thermal conductivity of rigid PUR foams is in the range from 0.018 up to 0.028 W/(m·K). The thermal conductivity factor of rigid PUR foams is two times lower than that of polystyrene, which is a widely used alternative material for insulation purposes [3].

Nowadays one of the problems facing the PUR industry is its dependence on petroleum-based raw materials. The synthesis of polymers from renewable resources has been investigated by leading research teams from different countries [4–8]. These studies have been motivated by a need for alternative raw materials, replacing the petrochemical resources which are running short. Investigations in the field of PUR are especially intensive. Interest in the use of renewable raw materials, in particular, non-food plant oils, polysaccharides, proteins, tannins, and lignin for PUR, is increasing [9–11].

Technical lignins and tall oil are generated in large scale as byproducts/wastes in pulp mills. Tall oil is a mix of different fatty (C12—C22) and rosin acids (C20). The synthesis of polyols from tall oil by esterification or amidization methods and PUR preparation afterwards is described as an environmentally friendly process with low energy consumption [12,13]. Lignin is the most abundant renewable phenolic polymer. The majority of technical lignin is burned as a cheap fuel to generate energy in pulp mills. However, it could be potentially used as a binder, plasticizer, sorbent, filler of composite materials, polymeric carrier of biologically active agents, additive for animal food preparations [14,15] and raw material for vanillin production [16]. At the same time, lignin is considered as a prospective antioxidant [17]. The activity of lignin as an antioxidant and the influence of the production process on it have been previously evaluated [18–21]. Nowadays different types of PUR production obtained from lignin are developed and described: rigid foams [22], flexible foams [23], films and coatings [24].

Corresponding author: aiga.paberza@gmail.com

During outdoor exposure, polymers chemically degrade due to the influence of short wavelength ultraviolet (UV) rays present in the solar spectrum. The service life of polymers in outdoor applications becomes limited due to weathering [25]. The weathering leads to a rapid decrease of the polymer's physical properties. This decrease is caused by a random scission of bonds in the polymer chain resulting in the formation of free-radicals, which migrate along the chain [26]. PUR made from an aromatic isocyanate will become yellow during exposure to UV light. The yellowing is caused by oxidation reaction in the backbone of the polymer. Irradiation decreases the physical and visual characteristics of PUR surface, which results in rapid color change and degradation [27].

The objective of this study was to obtain rigid PUR foams from renewable raw materials such as pulp mill byproducts, tall oil and lignin, and to evaluate long-term photodegradation as a result of UV irradiation. Fourier transform infrared spectroscopy (FTIR) is commonly used for investigation of PUR photodegradation. Besides FTIR, scanning electron microscopy (SEM), spectrophotometry and differential scanning calorimetry (DSC) analysis were used to study the photodegradation of rigid PUR foams.

2 EXPERIMENTAL

2.1 Materials

Lignopolyol (OH=445 mg KOH/g; H_2O=0.1 wt%; viscosity 20.1 Pa·s) and tall oil polyol (OH=273.9 mg KOH/g; H_2O=0.1 wt%; viscosity 2.1 Pa·s) were synthesized at Latvian State Institute of Wood Chemistry. Lupranol 3300 (OH=400 mg KOH/g; viscosity 0.54 Pa·s) and Lupranol 3422 (OH=490 mg KOH/g) are commercially available polyols from BASF. Lupranol 3300 is a trifunctional polyether polyol based on glycerine and Lupranol 3422 is a high functional polyether polyol based on sorbitol.

Lignopolyol was synthesized from organosolv lignin BIOLIGNIN™ and propylene oxide by oxypropylation reaction. The weight ratio was 70 wt% of BIOLIGNIN™ to 30 wt% of propylene oxide. As a catalyst 1.5 wt% KOH was used. The lignopolyol synthesis was carried out in a sealed reactor which was heated to 160-165°C till exothermic reaction starts. When reaction was over the KOH was neutralized by acetic acid. The obtained product was dissolved in dichloromethane and filtered. Dichloromethane was distilled off in vacuum evaporator. A more detailed description of lignopolyol synthesis is given by Arshanitsa et al. [28].

Tall oil polyol was synthesized from tall oil and diethanolamine by amidization reaction which was carried out at 145 ± 5°C. The molar ratio was 1 M of tall oil to 1.15 M of diethanolamine. This synthesis is described in more detail by Pietrzak et al. [29].

Amine catalyst Polycat 5 from Air Products and 30% solution of potassium acetate in diethylene glycol (KAc) from Performance Chemicals Handels GmbH were used as catalysts. Surfactant NIAX Silicone L6915 from Momentive Performance Materials was used as an additive to provide closed foam structures. Distilled water was used as a chemical blowing agent. Solkane 365/227 (87:13) from Solvay was used as a physical blowing agent. Polymeric diphenylmethane diisocyanate – IsoPMDI 92140 (PMDI) from BASF was used as an isocyanate component (w_{NCO} = 31.5%).

2.2 Preparation of Rigid PUR Foam Samples

Two different rigid PUR foams were obtained from renewable sources—tall oil polyol and lignopolyol. Also, rigid PUR foam sample was obtained from commercially available polyol Lupranol 3300. The PUR samples were named according to the main polyol used in their formulation: the "Lupr" from Lupranol 3300, the "TO" from tall oil polyol and the "LP" from lignopolyol. Rigid PUR foam formulation is presented in Table 1.

The PUR foams were obtained by free-rising method at room temperature. All raw materials, except isocyanate, were first mixed in a 500 mL plastic beaker. Then, the isocyanate was added and mixed for 15 s at a speed rate of 2000 rpm. After that the mixture was quickly poured into an open mold (20×30×10 cm). The height of foams was ~8–10 cm. The foams were conditioned at 20°C for 24 h. Afterwards the rigid PUR

Table 1 Rigid PUR foam sample formulation.

Raw material	Content, parts by weight		
Name	Lupr	TO	LP
Lupranol 3300	70	-	-
Tall oil amide	-	70	-
Lignopolyol	-	-	70
Lupranol 3422	30	30	30
KAc	0.8	0	0
Polycat 5	0.5	0.1	0.5
NIAX Silicone L6915	1.5	1.5	1.5
Water	0.5	0.5	0.5
Solkane 365/227 (87:13)	30	35	20
PMDI	131	107	142

foam samples (11×7×0.5 cm) for degradation test and samples for density and closed cell content (10×3.5×3.5 cm) were cut out.

2.3 Apparent Core Density and Closed Cell Content

In accordance with EN ISO 845:2006, the apparent core density of obtained rigid PUR foams (after all forming skin has been removed) was calculated as a ratio of the sample weight to the sample volume. Closed cell content of rigid PUR foam samples with dimension 10×3.5×3.5 cm was tested according to EN ISO 4590:2003.

2.4 Accelerated Degradation

Accelerated photodegradation was carried out in a UV accelerated weathering tester at 60°C temperature. A fluorescent lamp UVA-340 (295–420 nm, max 340 nm) with the intensity 0.89 W/m^2 was used. The degradation was performed for 1000 h. At 100 h, 200 h, 500 h, 850 h and 1000 h, samples were tested by spectrophotometer and SEM.

2.5 SEM Analysis

The cellular structures of PUR samples were characterized using SEM Tescan TS 5136 MM with secondary electron detector. The foam samples were cut into pieces of approximately 10×10×4 mm with a scalpel blade. It was done in order to cut surfaces as clean as possible. Samples were glued on aluminum specimen stubs and sputter coated with gold afterwards using sputter coater Emitech K550X (current 25mA, coating time 2 min). Obtained SEM images and data were processed with VEGA TC computer software. The thickness of degraded layer was measured. In order to determine the average size of cells and anisotropy, cell diameters in both the axial and transverse directions were measured. For each sample ~100 cell measurements were done.

2.6 DSC Analysis

Differential scanning calorimetry (DSC) analysis was carried out to study the glass transition temperature (T_g) variations. DSC was performed on a TA Instrument DSC Q1000 under nitrogen atmosphere using approximately 5 mg of each sample. Samples were initially heated from ambient temperature to 120°C at a heating rate of 10°C/min, cooling until −30°C and then heated again at a rate of 10°C/min to 200°C. The preheating step (from ambient temperature to 120°C) was done in order to remove the nonreversible thermal effects like release of inner tensions, change of macromolecular conformation and crosslinking due to traces of unreacted isocyanate.

2.7 Spectrophotometry

Color difference (ΔE) was measured using a CM-2500d spectrophotometer under D65 light source 10°, d/8°. The color difference calculation was performed based on CIE 1976 (L*a*b*) color difference equation:

$$\Delta E *_{a,b} = \sqrt{(L_2^* - L_1^*)^2 + (a_2^* - a_1^*)^2 + (b_2^* - b_1^*)^2} \qquad (1)$$

The subscript 1 means the values measured before UV exposure, while subscript 2 denotes the values measured after UV exposure. The $(a_2^* - a_1^*)$ positive values describe a red shift but negative – the green shift, $(b_2^* - b_1^*)$ positive values characterize the yellow shift, while negative values describe the blue shift [30].

2.8 FTIR Spectroscopy

The FTIR analysis was carried out for the initial samples (the PUR foam samples before exposure to UV irradiation) and for the samples after 1000 h exposure to UV irradiation.

The initial and irradiated samples were sliced ~2 mm and pressed by press with 10t/m^2. The FTIR spectra were recorded with Perkin-Elmer spectrometer, model: Spectrum One FT-IR spectrometer with an ATR polarization accessory. Scanning range from 4000 to 650 cm^{-1}, number of scans: 64, resolution: 4 cm^{-1}.

The total area of peaks at 1710 and 1510 cm^{-1} was calculated. The applied peak ranges for calculation are shown in Table 2. The peak area of aromatic ring vibration (1535 to 1492 cm^{-1}) was chosen according to Huang et al. [31]. By applying these peak ranges, the defined areas were always above the line connecting the limit wavenumbers of the range. The peak area of aromatic ring vibration (1535 to 1492 cm^{-1}) was chosen according to Huang et al. [32]. By applying these peak ranges, the defined areas were always above the line connecting the limit wavenumbers of the range.

Table 2 Range of peak area adopted for the calculation.

Peak total area	Range of peak area, cm^{-1}
S_{1710}	1820 – 1620*
S_{1510}	1535 – 1492

*The beginning and end of each peak was defined more precisely individually.

Also the total spectrum area (S_{total}) in the range of 4000 to 650 cm^{-1} was calculated for all spectra of initial and irradiated rigid PUR samples. The areas of normalized peaks were calculated by dividing measured peak area to total spectrum area (S_{1710}/S_{total} and S_{1510}/S_{total}).

3 RESULTS AND DISCUSSION

3.1 Apparent Core Density and Closed Cell Content of Rigid PUR Foams

Tall oil polyol, lignopolyol and commercial polyols were used as main polyols in the TO, LP and Lupr samples, respectively. Rigid PUR foams with the apparent core density in the range of ~35–40 kg/m^3 and with the closed cell content >95% were obtained (Table 3).

The apparent core density and closed cell content of obtained rigid PUR foams are suitable for application as thermal insulation material.

3.2 Renewable Material Content

The rigid PUR foams were also characterized by renewable material content. Renewable material content in the main polyol, polyol component and in the end product—rigid PUR foams—is shown in Table 4.

It is advantageous to use a slight excess of polyisocyanate to ensure an isocyanate index of 1.05–1.2. The excess of isocyanate improves the compressive strength of rigid PUR foams and shrinkage is lessened [33]. It is

Table 3 Apparent density and closed cell content of rigid PUR foams.

Sample	Apparent core density, kg/m^3	Closed cell content, %
Lupr	39.4 ± 1.0	96 ± 1
TO	35.0 ± 1.0	96 ± 1
LP	38.6 ± 1.0	95 ± 1

Table 4 Renewable content in the main polyol, polyol component and rigid PUR foams.

PUR sample	Renewable content in the main polyol, wt%	Renewable content in polyol component, wt%	Renewable content in foams, wt%
Lupr	0	0.4	0.2
TO	71.0	36.9	20.6
LP	30.0	17.7	8.2

possible to increase isocyanate index to get polisocyanurate foams but that decreases the renewable material content in foams. The isocyanate index (NCO/OH molar ratio) of 1.2 was chosen due to the fact that it allows the achievement of higher renewable material content in rigid PUR foams.

Renewable materials in the obtained rigid PUR foams are tall oil, lignin and water. The highest renewable material content showed rigid PUR foams from tall oil polyol (20.6%) since the renewable material content in polyol is high (71%). Accordingly, foams from lignopolyol have relatively small renewable material content (8.2%) due to low content of renewables in polyol (30%)

3.3 SEM Results

SEM images (Figure 1) were acquired before and after exposure to UV to study morphology of foams and to compare depth of degradation. The SEM images show that PUR foams have mainly closed cells. The SEM results correlate with the closed cell content results presented in Table 3. Degradation of the surface of foams appears when foams are exposed to UV irradiation. The membranes of cells collapse first but the network of struts remains. It can be assumed that cell
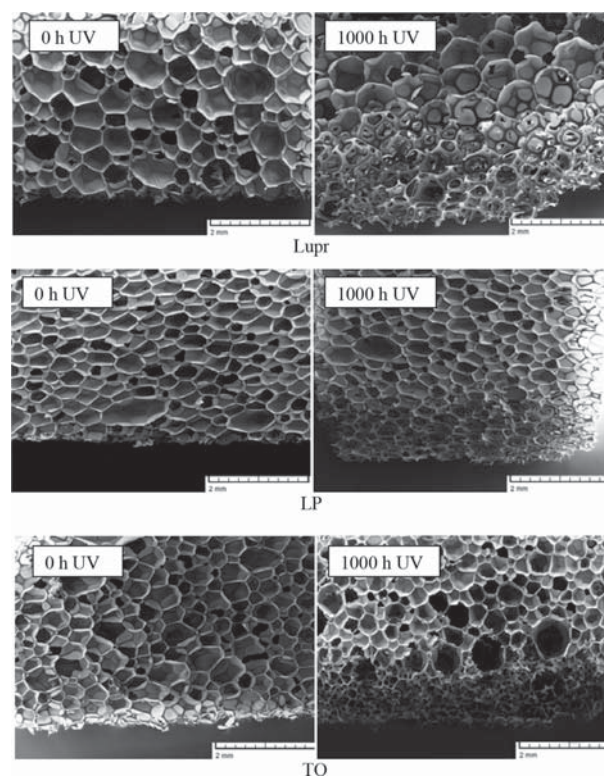

Figure 1 SEM images of the rigid PUR foams before and after the exposure to UV.
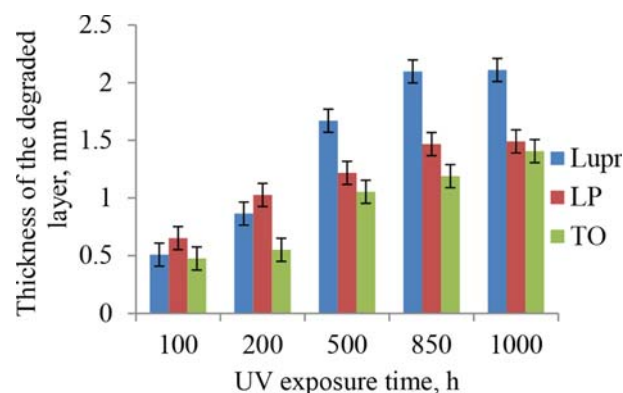
Figure 2 Thickness of the degraded layer versus UV exposure time.

membranes behave like thin PUR films, but struts are the thickest and most robust parts of the rigid foam. The degraded layer is clearly visible and therefore can be easily measured. Figure 2 presents the thickness of degraded layer during UV exposure.

Figure 2 shows that after 100 h the level of degradation is similar for all the samples. A slightly larger difference is observed after 200 h. With UV irradiation time of 500 h or longer, rigid PUR foams from commercial polyol Lupranol 3300 showed the thickest degraded layer. While the thickness of the degraded layer of PUR foams obtained from renewable materials (tall oil polyol and lignopolyol) was ~25% less.

The degradation level of rigid PUR foams is impacted not only by chemical structure of foams but also by cell morphology of rigid PUR foams. The cell size in both transverse and axial direction, as well as anisotropy coefficient, was determined from SEM images and is reported in Table 5. As can be seen from Table 5 and Figure 1, the cell size is larger and foams have almost round shaped cells (anisotropy coefficient 1.02) for PUR foams from Lupranol 3300. The cellular structure of PUR foams obtained from renewable materials is finer and elongated.

Since density for all samples are almost the same, differences in cell size can be partially explained by the high viscosity of renewable polyols. During the

Table 5 Average cell size of rigid PUR foam samples.

PUR sample	Average transverse cell size, μm	Average axial cell size, μm	Anisotropy coefficient
Lupr	570 ± 140	570 ± 130	1.02
TO	400 ± 70	510 ± 130	1.28
LP	340 ± 40	540 ± 90	1.56

Table 6 Variations of glass transition temperature of rigid PUR foams.

	T_g, °C (initial)	T_g, °C (irradiated)	The change of T_g, °C
Lupr	101	68	-33
TO	111	-	-
LP	119	96	-23

foaming process the polymer expansion is slow, causing the formation of smaller cells with larger cell size distribution, compared to systems where commercial polyol is used.

3.4 DSC Results

Results of the DSC analysis performed on the initial and UV-aged rigid PUR foams are reported in Table 6.

A significant variation of T_g is observed. It indicates the existence of degradation phase caused by UV irradiation. Rigid PUR foams from Lupranol 3300 showed the largest change in T_g, whereas a small change in T_g was observed for rigid PUR foams from lignopolyol.

The decrease of T_g reflects an increase of the free volume in the polymer, and it can be related to the decrease in molecular weight due to chain scissions caused by oxidation reactions [34,35].It was not possible to visualize clearly T_g by DSC analysis for irradiated rigid PUR foam from tall oil polyol. Other more sensitive methods should be used in further studies.

3.5 The Spectrophotometry Measurements

During UV irradiation the aromatic structures are oxidized in the central methylene group, leading to highly conjugated quinone products. The accumulation of quinone products due to the chain scission of the PUR macromolecules induces formation of colored products [32].

The formation of colored products of rigid PUR foams was analyzed using spectrophotometry. The total color difference $\Delta E^*_{a,b}$ of rigid PUR foams as a function of exposure time is shown in Figure 3.

The total color difference $\Delta E^*_{a,b}$ increased with increasing irradiation time. The PUR sample obtained using commercial polyol Lupranol 3300 showed the greatest yellowing. The smallest change in color was shown by LP sample, indicating that rigid PUR foams from LP show better stability against UV degradation.
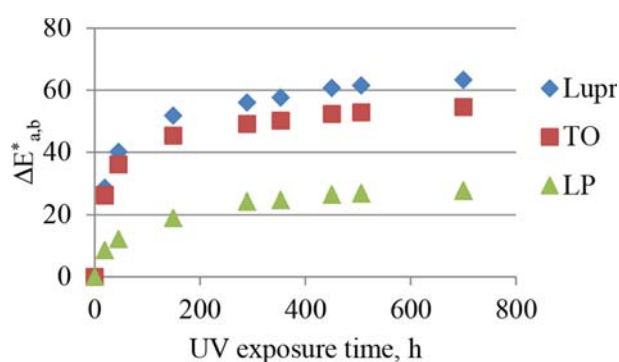
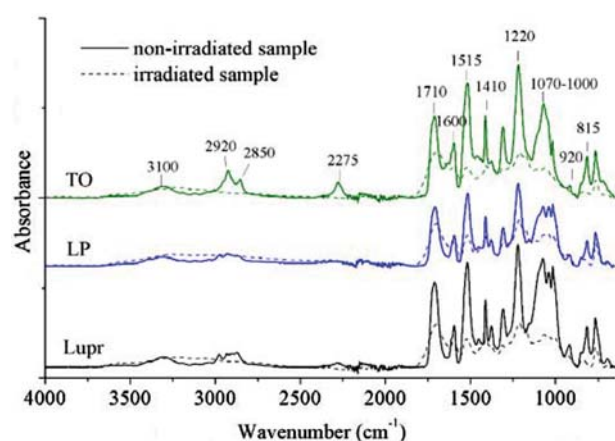**Figure 3** The total color difference ΔE*$_{a,b}$ versus the irradiation time.

Figure 4 FTIR spectra of the PUR before and after exposure to UV.

3.6 FTIR Measurements

The obtained rigid PUR foams were characterized by FTIR before and after 1000 h exposure to UV irradiation. The FTIR spectra of initial PUR samples and after photodegradation are shown in Figure 4.

All FTIR spectrum of initial PUR foam present a band at 3310 cm^{-1}, which corresponds to the stretching vibration of N–H group and –OH group. Asymmetric and symmetric CH$_2$ bands (at 2920 and 2850 cm^{-1}, respectively) are more intense for PUR foams obtained from tall oil polyol due to the long-chain linear aliphatic structure in polyol that was confirmed by the band at 720 cm^{-1} (methylene rocking vibration).

The peak at 2275 cm^{-1} corresponds to the free, unreacted isocyanate groups. After UV exposure the NCO group peak dissapears because UV radiation promotes chemical reactions in foam. The vibration band in the carbonyl region (1760–1660 cm^{-1}) can be considered as a sum of several peaks with near equal areas that corresponds to C=O vibration modes of various carbonyls found in urethanes, urea and ester moieties. Peaks at 1600, 1500, and 1410 cm^{-1} are suggestive of

aromatic –C=C– stretching vibrations [36]. The skeletal vibration of C=C in the aromatic ring from 1600 cm^{-1} is associated with the absorbance from 815 cm^{-1}, the last being characteristic to C–H out of plane bending vibration in 1,4–disubstituted aromatic ring. The 1410 cm^{-1} peak is specific to the trimer 6-membered ring which is an isocyanate trimerization product [37].

The band at 1310 cm^{-1} is attributable to the bending vibrations of CH$_3$ groups. The absorbance at 1515 cm^{-1} in the FTIR spectrum of rigid PUR foams could be attributed to the coupling of N–H bending vibration with C–N stretching vibration in the –C–NH group (amide II band), overlapping with previous mentioned aromatic –C=C– stretching vibrations at 1500–1510 cm^{-1}. The weaker vibration band at 1310 cm^{-1} corresponds to the combination between N–H bending vibration and C–N stretching vibration (amide III band) [38,39]. The FTIR spectrum of rigid PUR foam from tall oil polyol (polyester polyol) have less absorption bands in region 1070–1000 cm^{-1} that corresponds to C–O bonds of esters, ethers and hydroxyl groups and do not show highly individual bands comparing with rigid PUR foams from polyether polyols (lignopolyol and Lupranol 3300). Degradation at accelerated UV irradiation of rigid PUR foams obtained from Lupranol 3300, lignin and tall oil polyols are similar to previously described aromatic PUR photodegradation by Rosu et al. [27].

The FTIR difference spectra were employed to characterize the chemical structure of rigid PUR foams before and after UV irradiation. The FTIR difference spectra are the difference between spectra of irradiated samples and the spectra of initial rigid PUR foam samples. It is clearly visible that the intensity of absorbance decreases in almost all ranges of the spectrum after UV irradiation (Figure 5).

The positive absorbances of the difference FTIR spectra in Figure 5 reflect the structures that were formed
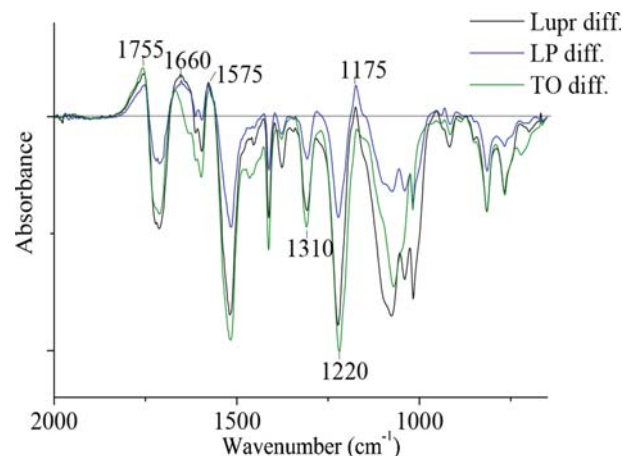

Figure 5 FTIR difference spectra of the rigid PUR foam samples.

as a result of UV action on rigid PUR foams. The negative absorbances show structures that were lost during the UV exposure (intensity of absorbance decreased). The positive absorbance at 1175 cm^{-1} can be attributed to the formation of crosslinks between the polyol segments [40–42]. It may also involve the PUR segments and, in particular, the reactivity of groups closed to the aromatic structures [40,43–45]. Negative band at 1220 cm^{-1} shows decreasing of C–O bonds. The conversion of the urethane bond into ortho-aromatic amine ester structure due to the photo-Fries rearrangement could explain the negative band at 1310 cm^{-1} (corresponds to the combination between N–H bending vibration and C–N stretching vibration).

The difference spectra show important modifications in the carbonyl stretching region (1800–1600 cm^{-1}) due to oxidation caused by UV radiation. The band in carbonyl region becomes wider but less intense, which refers to the new C=O containing structures (Figure 4). That gives positive absorbance at 1755 and 1660 cm^{-1} in the difference spectra (Figure 5). The band at 1660 cm^{-1} could be assigned to conjugated carbonyl, possible in quinone structure formed during photodegradation. The peaks at 1510, 1412, and 815 cm^{-1}, which are characteristic of the aromatic ring, decrease in all spectra. It shows that aromatic structures from PUR are not stable to light and are susceptible to rapid degradation during UV exposure.

The total peak area of carbonyl region and aromatic peak at 1510 cm^{-1} were calculated to quantitatively characterize the oxidation intensity of aromatic groups present in rigid PUR foams. Figure 6 shows the normalized peaks areas (S_{1710}/S_{total} and $S_{1510}/S_{total})$ of initial and irradiated rigid PUR foams.

As mentioned before, the decrease of absorbance intensity in region 1535–1492 cm^{-1} shows the degradation of aromatic structures. Rigid PUR foam from lignopolyol showed the smallest difference in both S_{1510}/S_{total} and S_{1710}/S_{total}. This indicates the least degradation of aromatic structures, which correlates with
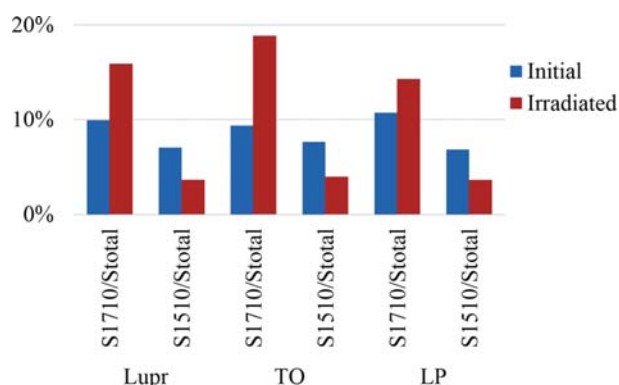
the results of spectrophotometry (the smallest color change) and SEM (the thinnest degraded layer).

4 CONCLUSIONS

In rigid polyurethane foams prepared from polyols obtained from the pulp production byproducts of tall oil and lignin, renewable material content in foams reached 21% and 8% respectively. Also, rigid polyurethane foams from commercially available polyol were obtained as a comparison material.

Photodegradation of rigid polyurethane foams was carried out. Our studies proved that polyurethane foam degradation greatly depends on the polyol used in its formulation. Our results showed that replacing commercial polyol with tall oil- and lignin-based polyols decreased the photodegradation by 25% (corresponding to the results of the thickness of the degraded layer). The results of spectrophotometry and FTIR showed that rigid polyurethane foams from lignopolyol have the least oxidation of aromatic structures.

Not only is the use of renewable materials desirable for producing rigid PUR foams, but their improved resistance to UV degradation can also provide added-value products in the polyurethane market.

ACKNOWLEDGMENTS

REFERENCES

1. M.C. Silva, J.A. Takahashi, D. Chaussy, M.N. Belgacem, and G.G. Silva, Composites of rigid polyurethane foam and cellulose residue. *J. Appl. Polym. Sci.* **117**, 3665–3672 (2010).

2. U. Stirna, I. Beverte, V. Yakushin, and U. Cabulis, Mechanical properties of rigid polyurethane foams at room and cryogenic temperatures. *J. Cell. Plast.* **47**(4), 34–355 (2011).

3. W. Zatorski, Z.K. Brzozowski, and A. Kolbrecki, New developments in chemical modification of fire-safe rigid polyurethane foams. *Polym. Degrad. Stab.* **93**(11), 2071–2076 (2008).

4. K. Hill, Fats and oils as oleochemical raw materials. *Pure Appl. Chem.* **72**(7), 1255–1264 (2000).

5. L. Montero de Espinosa and M.A.R. Meier, Plant oils: the perfect renewable resource for polymer science. *Eur. Polym. J.* **47**(5), 837–852 (2011).

Figure 6 Normalized aromatic and carbonyl peaks areas.

6. C.K. Williams and M.A. Hillmyer, Polymers from renewable resources: a perspective for a special issue of polymer reviews. *Polym. Rev.* **48**(1), 1–10 (2008).

7. A. Gandini, Polymers from renewable resources: a challenge for the future of macromolecular materials. *Macromolecules* **41**(24), 9491–9504 (2008).

8. J. Van Haveren, E.L. Scott, and J. Sanders, Bulk chemicals from biomass. *Biofuels, Bioprod. Biorefin.* **2**(1), 41–57 (2008).

9. M.E. Espinosa and M.A.R. Meier, Plant oils: the perfect renewable resource for polymerscience. *Eur. Polym. J.* **47**, 837–852 (2011).

10. A. Gandini, The irruption of polymers from renewable resources on the scene of macro-molecular science and technology. *Green Chem.* **13**, 1061–1083 (2011).

11. J.M. Raquez, M. Deléglise, M.F. Lacrampe, and P. Krawczak, Thermosetting (bio)materials derived from renewable resources: a critical review. *Prog. Polym. Sci.* **35**, 487–509 (2010).

12. V. Yakushin, U. Stirna, O. Bikovens, M. Misane, I. Sevastyanova, and D. Vilsone, Synthesis and characterization of novel polyurethanes based on tall oil. *Materials Science - Medžiagotyra*. **19**(4), 390–396 (2013).

13. U. Cabulis, M. Kirpluks, U. Stirna, M.J. Lopez, M.C. Vargas-Garcia, F. Suárez-Estrella, and J. Moreno, Rigid polyurethane foams obtained from tall oil and filled with natural fibers: Application as a support for immobilization of lignin-degrading microorganisms. *J. Cell. Plast.* **48**(6), 500–515 (2012).

14. T.Q. Hu. *Chemical Modification, Properties, and Usage of Lignin*, Kluwer Academic/Plenum Publishers, New York (2002).

15. L. Glasser, S. Sarkanen, *Lignin: Properties and Materials*, American Chemical Society, Washington, DC (1989).

16. E.A.B. da Silva, M. Zabkova, J.D. Araujo, C.A. Cateto, M.F. Barreiro, M.N. Belgacem, and A.E. Rodrigues, An integrated process to produce vanillin and lignin-based polyurethanes from Kraft lignin. *Chem. Eng. Res. Des.* **87**, 1276–1292 (2009).

17. A. Arshanitsa, J. Ponomarenko, T. Dizhbite, A. Andersone, R.J.A. Gosselink, J. van der Putten, M. Lauberts, and G. Telysheva. Fractionation of technical lignins as a tool for improvement of their antioxidant properties. *J. Anal. Appl. Pyrolysis* **103**, 78–85 (2013).

18. A. García, A. Toledano, M.A. Andrés, and J. Labidi, Study of the antioxidant capacity of Miscanthus sinensis lignins, *Process Biochem.* **45**, 935–940 (2010).

19. Q. Lu, W. Liu, L. Yang, Y. Zu, B. Zu, M. Zhu, Y. Zhang, X. Zhang, R. Zhang, Z. Sun, J. Huang, X. Zhang, and W. Li, Investigation of the effects of different organosolv pulping methods on antioxidant capacity and extraction efficiency of lignin, *Food Chem.* **131**, 313–317 (2012).

20. R. Bhat, H.P.S.A. Khalil, and A.A. Karim, Exploring the antioxidant potential of lignin isolated from black liquor of oil palm waste, *C. R. Biol.* **332**, 827–831 (2009).

21. A. García, M.G. Alriols, G. Spigno, and J. Labidi, Lignin as natural radical scavenger. Effect of the obtaining and purification processes on the antioxidant behaviour of lignin. *Biochem. Eng. J.* **67**, 173–185 (2012).

22. C.A. Cateto, M.F. Barreiro, C. Ottati, M. Lopretti, A.E. Rodrigues, and M.N. Belgacem, Lignin-based rigid polyurethane foams with improved biodegradation. *J. Cell. Plast.* **50**(1), 81–95 (2014).

23. P. Cinelli, I. Anguillesi, and A. Lazzeri, Green synthesis of flexible polyurethane foams from liquefied lignin. *Eur. Polym. J.* **49**, 1174–1184 (2013).

24. C. Ciobanu, M. Ungureanu, L. Ignat, D. Ungureanu, and V.I. Popa, Properties of lignin–polyurethane films prepared by casting method. *Ind. Crop. Prod.* **20**, 231–241 (2004).

25. A. Davis and N. Grassie, *The weathering of polymers in development in polymer degradation*, Applied Science Publishers, London (1977).

26. R.P. Singh, N.S. Tomer, and S.V. Bhadraiah, Photo-oxidation studies on polyurethane coating: effect of additives on yellowing of polyurethane. *Polym. Degrad. Stab.* **73**, 443–446 (2001).

27. D. Rosu, L. Rosu, and C.N. Cascaval, IR-change and yellowing of polyurethane as a result of UV irradiation. *Polym. Degrad. Stab.* **94**, 591–596 (2009).

28. A. Arshanitsa, A. Paberza, L. Vevere, U. Cabulis, and G. Telysheva, Two approaches of introduction of wheat straw lignin in rigid polyurethane foams, *AIP Conference Proceedings*, Volume 1593 (388), pp. 388–391 (2014).

29. K. Pietrzak, M. Kirpluks, U. Cabulis, and J. Ryszkowska. Effect of the addition of tall oil-based polyols on the thermal and mechanical properties of ureaurethane elastomers. *Polym. Degrad. Stab.* **108**, 201–211 (2014).

30. N. Pauler. *Paper optics*, AB Lorentzen & Wettre, Kista (2002).

31. X.F. Yang, D.E. Tallman, G.P. Bierwagen, S.G. Croll, and S. Rohlik, Weathering degradation of a polyurethane coating. *Polym. Degrad. Stab.* **74**, 341–351 (2001).

32. C. Wilhelm, A. Rivaton, and J.L. Gardette. Infrared analysis of the photochemical behaviour of segmented polyurethanes. 3. Aromatic diisocyanate based polymers. *Polymer.* **39**, 1223–1232 (1998).

33. M. Szycher. *Szycher's Handbook of Polyurethanes, Second Edition.*, CRC press, USA (2012).

34. E. Pellizzi, A. Lattuati-Derieux, B. Lavédrine, H. Cheradame. Degradation of polyurethane ester foam artifacts: Chemical properties, mechanical properties and comparison between accelerated and natural degradation. *Polym. Degrad. Stab.* **107**, 255–261 (2013).

35. A. Boubakri, N. Guermazi, K. Elleuch, and H.F. Ayedi, Study of UV-aging of thermoplastic polyurethane material. *Mat. Sci. Eng. A-struct.* **527**, 1649–1654 (2010).

36. L. Li, R. Ma, N. Iyi, Y. Ebina, K. Takada, and T. Sasaki, Hollow nanoshell of layered double hydroxide. *Chem. Commun.* **29**, 3125–3127 (2006).

37. An isocyanate trimerisation catalyst system, a precursor formulation, a process for trimerising isocyanates, rigid polyisocyanurate/polyurethane foams made therefrom, and a process for making such foams, (July 27, 2011).

38. R.M. Silverstein, F.X. Webster, and D.J. Klemie. *Spectrometric identification of organic compounds, seventh edition*, John Willey & Sons, New York (2005).

SP

39. B. Stuart, *Infrared spectroscopy. Fundamental and applications*, John Wiley & Sons, New York (2004).

40. E. Cipriani, P. Bracco, S.M. Kurtz, L. Costa, and M. Zanetti, In-vivo degradation of poly(carbonate-urethane) based spine implants. Polym. Degrad. Stab. 98(6), 1225–1235 (2013).

41. E.M. Christenson, J.M. Anderson, and A. Hiltner, Oxidative mechanisms of poly(-carbonate urethane) and poly(ether urethane) biodegradation: in vivo and in vitro correlations. J. Biomed. Mater. Res. Part A. 70A(2), 245–55 (2004).

42. S. Fare, P. Petrini, A. Motta, A. Cigada, and M.C. Tanzi. Synergistic effects of oxidative environments and mechanical stress on in vitro stability of polyetherurethanes and polycarbonateurethanes. J. Biomed. Mater. Res. 45(1), 62–74 (1999).

43. T. Servay, R. Voelkel, H. Schmiedberger, and S. Lehmann, Thermal oxidation of the methylene diphenylene unit in MDI-TPU. Polymer 41(14), 5247–5256 (2000).

44. D.A. Wrobleski, D.A. Langlois, E. Bruce Orler, A. Labouriau, M. Uribe, R. Houlton, J.D. Kress, and B. Kendrick, Accelerated aging and characterization of a plasticized poly(ester urethane) binder. In: M. C. Celina, J. S. Wiggins, N. C. Billingham, editors. Polymer degradation and performance. American Chemical Society, Washington, pp. 181–196 (2009).

45. C.E. Hoyle, H. Shah, and K. Moussa. Photolysis of methylene 4,4'-diphenyldiisocya-nate-based polyurethane ureas and polyureas. In: R.L. Clough, N.C. Billingham, K.T. Gillen, editors. Polymer durability. American Chemical Society, Washington, pp. 91–111 (1996).